

“The Modification and Application of a Time Dependent Performance Prediction Model on the Dynamic Behaviour of a Sailing Yacht”

by

Bart Verwerft ¹

Alexander (J A) Keuning²

Notations:

α	angle of attack	C_{hull}	hull influence coefficient
β	leeway angle	C_{heel}	heel influence coefficient
β_0	zero lift drift angle	C_L	lift coefficient
δ_r	rudder angle	Fn	Froude Number
Φ	down wash angle	q	dynamic pressure
Λ	sweep back angle of the foil	Sc	wetter surface of the canoe body
φ	heel angle	Tc	draft of the canoe body
ψ	yaw angle	Vs	speed through the water of the yacht
AR_e	effective aspect ratio of the foil	$\frac{dC_L}{d\alpha}$	lift curve slope
b_k	span of the keel		
B_{wl}	waterline beam		

1. Introduction

The introduction by Keuning, Vermeulen and De Ridder in 2005 Ref [1] of a time domain simulation model, for the maneuvering behavior of a sailing yacht with the calculations of all the necessary coefficients in the equations of motions based solely on the results obtained from the Delft Systematic Yacht Hull Series (DSYHS), introduced the opportunity to formulate a time dependent solution of the equations of motion describing the equilibrium of an arbitrary sailing yacht or simulate the reaction of an arbitrary sailing yacht in changing environmental conditions. The development of such a simulation tool is often referred to as the development of a “dynamic VPP”, this in contrast to the “stationary” VPP.

In 2007 Keuning and Katgert Ref [2] already showed the possible beneficial application of this simulation model for the improvement of the tacking procedure of an IACC sailing yacht and Battistin and Ledri showed in a similar application the results for an IMS racing yacht in Ref [3].

This development now opens the opportunity to compare the results of the Velocity Prediction Program (VPP), with either a “stationary” or “steady state” true wind input with, using the same set of equations of motions, the (more) dynamic input of a varying true wind. The implicit assumption being that the later corresponds more to the realistic conditions found in the real sailing environment.

If the performance of all yachts is affected by the changing environmental conditions in the exactly the same way and to exactly the same amount, this is only of academic interest. If however it turns out that yachts, different by their prime design parameters, behave different in and react differently to changing conditions it becomes of more practical interest.

So the aim of the present study was to investigate some of these possible differences by comparing the results for stationary and the dynamic inputs in the dynamic VPP for a variety of changing conditions and a variety of yachts.

To be able to do this some of the formulations in the dynamic VPP, as originally formulated by Keuning e.a. in Ref [1], had to be reformulated to better suite the present applications in mind. In addition an entirely new approach to the side force formulation of the hull and its appendages has been derived. This new formulation overcomes the somewhat inconsistent approach as it was

¹ MSc student Delft Shiphidromechanics Department, Delft University of Technology

² Associate Professor Delft Shiphidromechanics Department, Delft University of Technology

used in the original model between the upright (no heel) and the heeled conditions and yields a better result in particular to the yaw moment developed by the hull and appendages, which is of prime interest in the maneuvering behavior of the yachts. The results of this development and some results of the applications will be presented in this paper.

2. Further development of the model

2-1 Modifications of the model to suite the present project.

Most modifications to the original model are in the aerodynamic formulations, used to calculate the sail forces.

In the original model as formulated by Keuning and Vermeulen Ref [1] no provisions were made for a varying true wind speed and a varying true wind direction. For the present study the provision to do it was considered essential to be able to introduce time dependent true wind speed and true wind direction. Also the possibility to simulate the behaviour of the yachts in a broad range of true wind directions was considered essential. The original model could only handle upwind scenarios. The primary aim of the original research by Keuning and Vermeulen was to formulate a model for the upwind sail balance of a wide variety of (mega) ships. So their main interest was in upwind conditions. Also in the later extension by Keuning and Katgert as presented in Ref [2] for the IACC yacht the primary focus was still on upwind sailing conditions and the associated tacking manoeuvres.

For the present study however it was considered to be important to be able to include a wider range of true wind angles and a varying true wind, both in speed and direction, to be able to compare the results of the static versus dynamic VPP's in a wide range of conditions, because the differences between the two solutions could very well be dependent on this.

So these adaptations to the code have been made. In general the formulations of the IMS sail force model have been used for the calculations and the in frame of this report for the sake of available space, reference is made to the more recent associated reports on this subject by various authors, amongst others, Claughton Ref [10], Cambell Ref [11], Ranzenbach Ref [12] and Fossati Ref [13] and documentations released by the ORC. It should be noted however that at present the model only accounts for the use of a mainsail and a jib.

In addition the possibility is introduced to use a true wind history as obtained from full scale measurements as an input file for the simulations.

In the hydrodynamic model no significant changes have been made. It should be noted however, that the new possibility to sail the boat at broader true wind angles, introduces the possibility of much higher boat speeds to be attained. Special attention therefore has been paid to the validity of the used expressions at these higher forward velocities. Also the yaw moment introduced by the off-centrelines position of the trust force generates a very large yaw moment in the broad reach and downwind conditions, when no spinnaker or poled out jib is taken into account. In the aero model at present only the offset due to heel is used and no attempt has been made to formulate the additional yaw moment due to slacking of the main sheet.

Another modification is the inclusion of different auto pilots to sail the ship in the simulations. In the original model only pre-described rudder scenarios have been used. Because true wind changes and scenarios may now be introduced a simple straight course keeping algorithm with constant helm does no longer suffice. The model was therefore extended with different auto pilot controls, keeping the yacht either at a constant course, constant apparent wind angle or true wind angle.

The autopilots in the model all have a similar structure, in which the input is the instantaneous course difference and course difference velocity. According to:

$$\delta_r^{n+1} = \delta_r^n + c_1 * (\Psi^{n+1} - \Psi_{set}) + c_2 * (\dot{\Psi}^{n+1})$$

where:

- δ_r^{n+1} : new rudder angle
- δ_r^n : rudder angle of the previous time step
- Ψ^{n+1} : heading of the yacht
- $\dot{\Psi}^{n+1}$: yaw velocity of the yacht

The coefficients c_1 and c_2 are determined considering the application in mind.

2-2 New side force model for the hull and appendages

In the original model the total side force of the hull and appendages and the separate contributions of hull, keel and rudder, are assessed differently in the upright and the heeled conditions:

In the upright condition the so called Extended Keel Method, as derived by Gerritsma Ref [4], is used to calculate the side force on keel and rudder, in which the side force generated by the hull is accounted for by the virtually extended keel inside the canoe body to the waterline. The downwash angle on the rudder is approximated as 50% of the leeway angle and the water velocity over the rudder reduced by 10% to account for the wake of the keel.

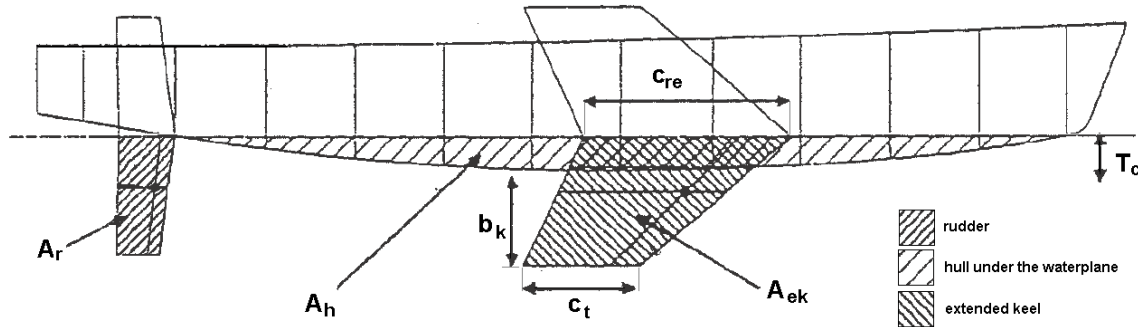


Figure 1: Definitions in the extended keel method

The total side force is calculated as the sum of the force on extended keel and rudder according to:

$$Y_{total} = Y_{ek} + Y_r$$

$$Y_{ek} = \frac{1}{2} \rho V_s^2 A_{ek} \left(\left(\frac{\partial C_L}{\partial \alpha} \right)_{ek} \beta \right)$$

$$Y_r = \frac{1}{2} \rho (0,9 V_s)^2 A_r \left(\left(\frac{\partial C_L}{\partial \alpha} \right)_r 0,4 \beta \right)$$

In which:

Y_{total} :	<i>the total side force in the horizontal plane</i>	[N]
Y_{ek} :	<i>the side force generated by the extended keel</i>	[N]
Y_r :	<i>the side force generated by the rudder</i>	[N]
A :	<i>The lateral area of the foil</i>	[m ²]
$\left(\frac{\partial C_L}{\partial \alpha}\right)$:	<i>the lift curve slope of the foil</i>	[deg ⁻¹]

The full yaw moment in this upright condition is calculated using the side force on keel and rudder with their respective separations to the centre of gravity of the ship and adding the yaw moment on the hull originating from the so called Munk moment. This procedure is fully developed and described by Keuning and Vermeulen in Ref [5].

Under heel this procedure does not work. Therefore in these conditions the results of the side force polynomial as derived from the results of the DSYHS by Keuning and Sonnenberg Ref [6] are used. This polynomial accounts for effects of heel angle and forward speed on the total side force production.

$$Fh \cos(\phi) = \left(b_1 \frac{T^2}{Sc} + b_2 \left(\frac{T^2}{Sc} \right)^2 + b_3 \frac{Tc}{T} + b_4 \frac{Tc}{T} \frac{T^2}{Sc} \right) \frac{1}{2} \rho V_s^2 Sc (\beta - \beta_{Fh:0})$$

$$\beta_{Fh:0} = B_3 \phi^2 Fn$$

in which:

$Fh \cos(\phi)$:	<i>the side force in the horizontal plane</i>	[N]
$\beta_{Fh:0}$:	<i>the zero lift drift angle</i>	[deg]
T :	<i>the total draft of hull with keel</i>	[m]
T_c :	<i>the draft of the canoe body</i>	[m]
Sc :	<i>the wetted surface of the canoe body</i>	[m]
Fn :	<i>the Froude Number</i>	[-]

and:

$$B_3 = 0,0092 * \left(\frac{Bwl}{Tc} \right) \left(\frac{Tc}{T} \right)$$

The coefficients b_1 to b_4 are presented as functions of the heeling angle between 0 and 30 degrees of heel.

The use of this expression yields however no information on the contribution of the three different components, i.e. hull, keel and rudder and therefore no result for the yaw moment can be found. To overcome this problem the distribution over keel and rudder as found in the upright condition is used in the heeled condition also. The Munk moment on the hull is calculated taking the geometry of the heeled hull in account. This procedure is also described in Ref [5]. Keuning, Katgert and Vermeulen Ref [7] improved the prediction of the side force production for higher aspect ratio keels and the yaw moment under heel by taking the newly derived formulation for the influence of the downwash of the keel on the rudder into the calculations.

This situation of using two different approaches was considered undesirable and inconsistent. So in the framework of the present study a new method has been developed.

In this new method the side force generated by keel and rudder is calculated using the expression derived by Whicker and Fehlner (W&F) for thin airfoils Ref [8]. This expression reads

$$\frac{d C_L}{d \alpha} = \frac{a_0 AR_e}{\cos \Lambda \sqrt{\frac{AR_e^2}{\cos^4 \Lambda} + 4 + \frac{57,3 a_0}{\pi}}}$$

In which:

$$\begin{aligned} AR_e &: \text{the effective aspect ratio} && [m] \\ \Lambda &: \text{the sweepback of quarter - chord line} && [rad] \\ \alpha &: \text{angle of attack} && [deg] \\ a_0 &: \text{the corrected section lift curve slope} && [-] \\ & & & a_0 = 0,9 \left(\frac{2\pi}{57,3} \right) \text{ per degree} \end{aligned}$$

In the present calculation the foils are not extended to the free surface, but taken at their actual size. The effect of the hull on the side force generation is formulated separately.

The end plate effect of the hull on the keel is generally taken into account by taken for the effective aspect ratio of the wing the double value of the geometrical aspect ratio of the wing, according to:

$$AR_e = 2 AR_{geo} = 2 \frac{b}{c_{mean}}$$

In which:

$$\begin{aligned} AR_e &: \text{the effective aspect ratio} && [-] \\ AR_{geo} &: \text{the geometric aspect ratio} && [-] \\ c_{mean} &: \text{mean geometric chord} && [m] \\ b &: \text{span of the foil} && [m] \end{aligned}$$

This is not the only effect of the presence of the hull. There is also the “lift carry over” from keel to the hull. From earlier measurements it was already found that the lift generated by the bare hull of a sailing yacht is generally small, so the main effect must be in the lift carry over from keel to hull. In an attempt to capture this lift carry over the ratio between the entire lift of the appended hull and the lift generated by the keel and rudder as calculated by using W&F expression is determined for the DSYHS. This ratio is further referred to as **hull influence coefficient** c_{hull} i.e.:

$$c_{hull} = \frac{L_t}{(L_k + L_r)}$$

In which:

$$\begin{aligned} c_{hull} &: \text{the hull influence coefficient} && [-] \\ L_t &: \text{the total measured hydrodynamic lift of the yacht} && [N] \\ L_r &: \text{the calculated lift of the rudder (with end plate)} && [N] \\ L_k &: \text{the calculated lift of the keel (with end plate)} && [N] \end{aligned}$$

This c_{hull} is now determined for the hulls of the DSYHS for the upright condition and this looks like the result depicted in Figure 2.

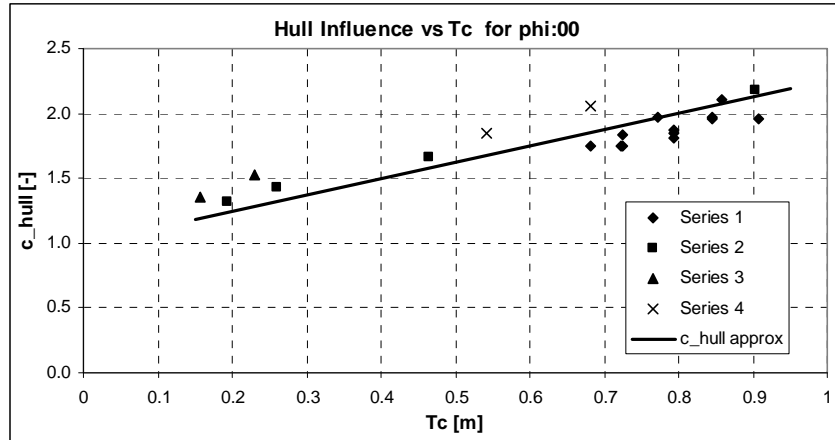


Figure 2: Hull influence coefficients vs. canoe body draft

The relation following for this approach for the keels and hulls in the DSYHS yields the following expression:

$$c_{hull} = a_0 Tc + 1 \quad \text{with: } a_0 = 1.25$$

To extend the range of application of this expression to keels with other plan forms (i.e. aspect ratios) the results of the Delft Various Keel Series (DVKS) and the Delft Systematic Keel Series (DSKS), as previously described by Keuning and Binkhorst in Ref [9] and Keuning and Sonnenberg in Ref [6], are used.

This yields the following dependency and formulation for the hull influence coefficient in the upright condition (Figure 3):

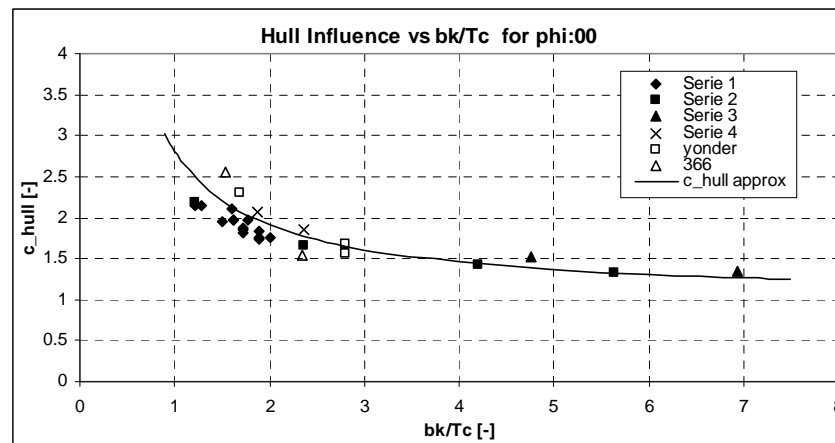


Figure 3: Hull influence coefficient vs. b_k/Tc ratio

With:

$$c_{hull} = 1,8 \frac{Tc}{bk} + 1$$

Now the influence of the heeling angle on the lift has to be taken into account. The influence of the heel angle on the lift production is captured by two mechanisms: one is the lift curve slope reduction due to the fact that the foils are brought closer to the free surface expressed as **heel influence coefficient** c_{heel} , the second one is the **zero lift drift angle** β_0 , which originates from the asymmetry of the hull when heeled. This asymmetry introduces a “negative” angle of attack on the appendages, which increases with heel angle and the beam to draft ratio in particular. This implies that the effective angle of attack on the appendages is reduced with this β_0

At first based on the results of the DSYHS, the DVKS and the DSKS a linear relation between the reduction of the lift curve slope and the heel angle due to the free surface effect is assumed. The results also show a moderate dependency on B/T ratio and forward speed, but for the time being this effect is neglected and shifted to future research. So in the present study for this effect of heel the following expression is used:

$$c_{heel} = 1 - b_0 \phi \quad \text{with: } b_0 = 0.382 \text{ for } \phi: [rad]$$

Also using the results of the above mentioned series an expression has been found for the zero lift drift angle, which shows reasonable agreement with the measured results. This expression reads:

$$\beta_0 = \left(c_0 \frac{B_{wl}}{T_c} \phi \right)^2 \quad \text{with: } c_0 = 0.405 \text{ for } \phi: [rad]$$

For the present research the forward speed influence on the lift curve slope has been neglected.

Finally the downwash angle of the keel on the rudder is approximated using the expression as formulated by Keuning, Katgert and Vermeulen in Ref [7].

$$\Phi = a_0 \sqrt{\frac{C_{Lk}}{AR_{e_k}}}$$

In which:

Φ : the downwash angle at the rudder [rad]

AR_e : the effective aspect ratio of the keel [-]

C_{Lk} : the lift coefficient of the keel [-]

phi	0°	15°
a ₀	0,136	0,137

The lift production of the keel is now calculated as follows:

$$Lc_{keel} = Lk_{W \& F} c_{hull} c_{heel}$$

$$Lk_{W \& F} = \left(\frac{dC_L}{d\alpha} \right)_{(W \& F)} \alpha_{e_{keel}} \frac{1}{2} \rho V_{e_{keel}}^2 A_{lat_{keel}}$$

In which:

$$V_{e_{keel}} = \sqrt{(-v - x_k \dot{\Psi} + (0,43 b_k + T_c) \dot{\phi})^2 + u^2}$$

$$\alpha_{e_{keel}} = \text{atan} \left(\frac{(-v - x_k \dot{\Psi} + (0,43 b_k + T_c) \dot{\phi})}{u} \right) - \beta_0$$

Along the same lines the lift production on the rudder is calculated using the following formula, now including the effect of the downwash of the keel:

$$Lc_{rudder} = Lr_{W \& F} c_{hull} c_{heel}$$

$$Lr_{W \& F} = \left(\frac{dC_L}{d\alpha} \right)_{(W \& F)} \alpha_{e rudder} \frac{1}{2} \rho V_{e rudder}^2 A_{lat rudder}$$

in which:

$$V_{e rudder} = \sqrt{(-v - x_r \dot{\Psi} + (0,43 b_r) \dot{\phi})^2 + u^2}$$

$$\alpha_{e rudder} = \text{atan} \left(\frac{(-v - x_r \dot{\Psi} + (0,43 b_r) \dot{\phi})}{u} \right) - \beta_0 - \Phi - \delta_r$$

The yaw moment is calculated using the side forces generated by the individual components and multiplying it with the distance of the corresponding centre of effort to the centre of gravity of the yacht. The yaw moment of the hull is calculated by taking the Munk moment over the entire length of the hull both upright and heeled as described by Keuning and Vermeulen in Ref [5].

The results of the new approach for the side force and the yaw moment calculation of the hull have been compared with the results of the previous method by Keuning and Vermeulen. In general it was found that the results of the new method show comparable correlation with the measurements as the results obtained with the old method.

This implies however that the new method is preferred due to its higher consistency over the heel angle. An important improvement is also found in the fact that now in both the upright and the heeled condition the actual area of the keel and rudder is taken into the side force calculations, while in the earlier expression only the effective draft of the keel was considered. Changes in the chord were not considered. Also improvements in the method may be expected when more of the available data is taken into account then in the present project. This extension is foreseen in the future.

Some typical results of the different approaches are depicted in Figure 4 to Figure 7.

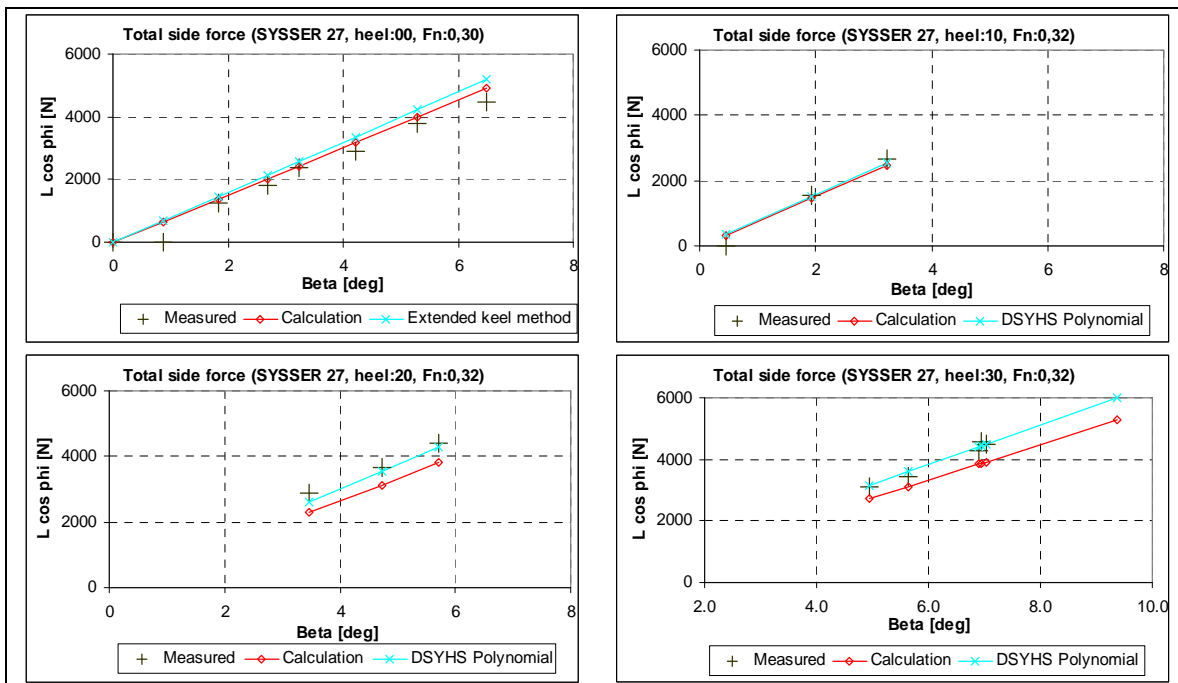


Figure 4: Measured and calculated total hydrodynamic side forces vs. leeway for SYSSER 27

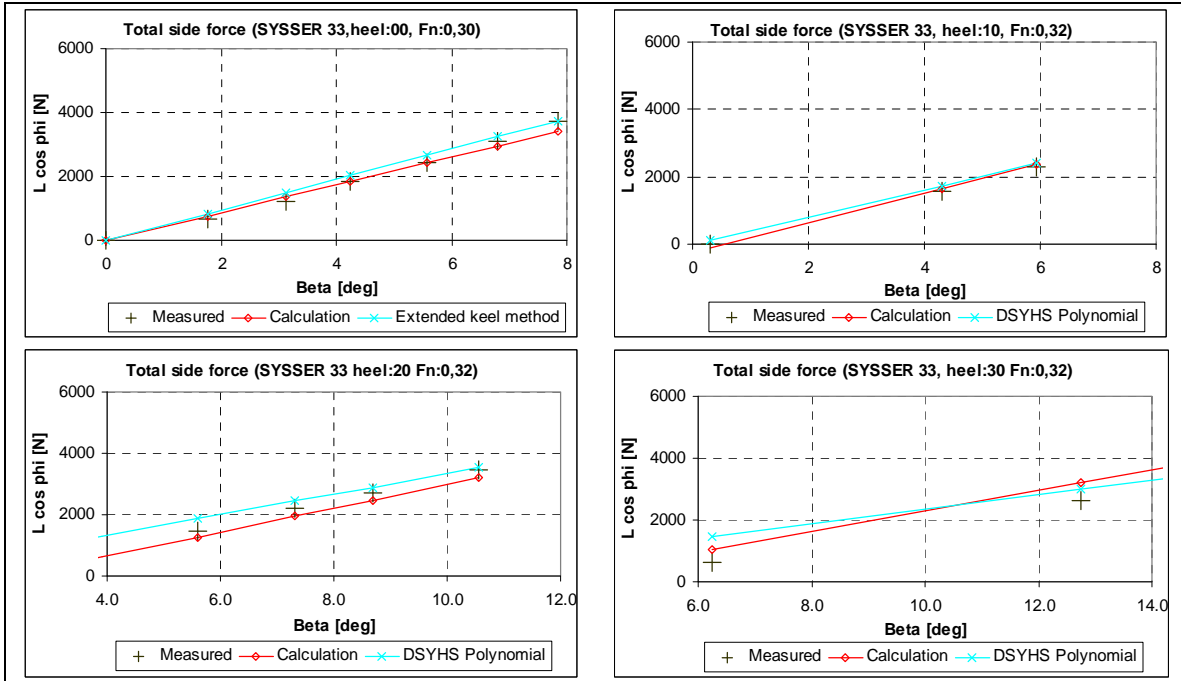


Figure 5: Measured and calculated total hydrodynamic side force vs. leeway for SYSSER 33

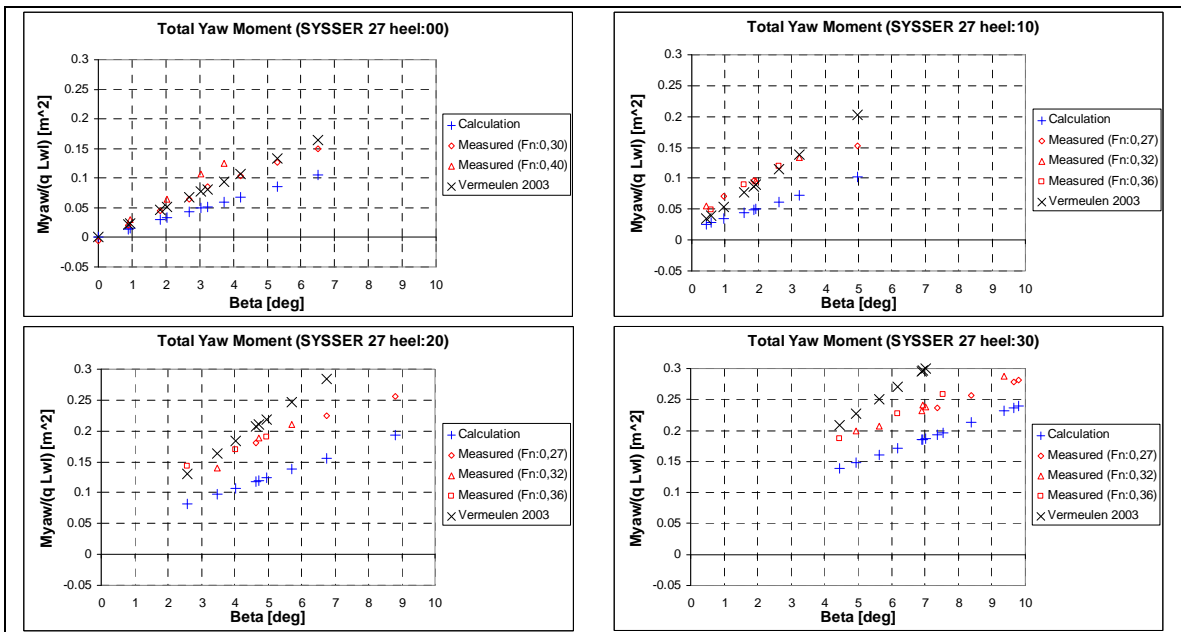


Figure 6: Measured and calculated total hydrodynamic yaw moment vs. leeway for SYSSER 27

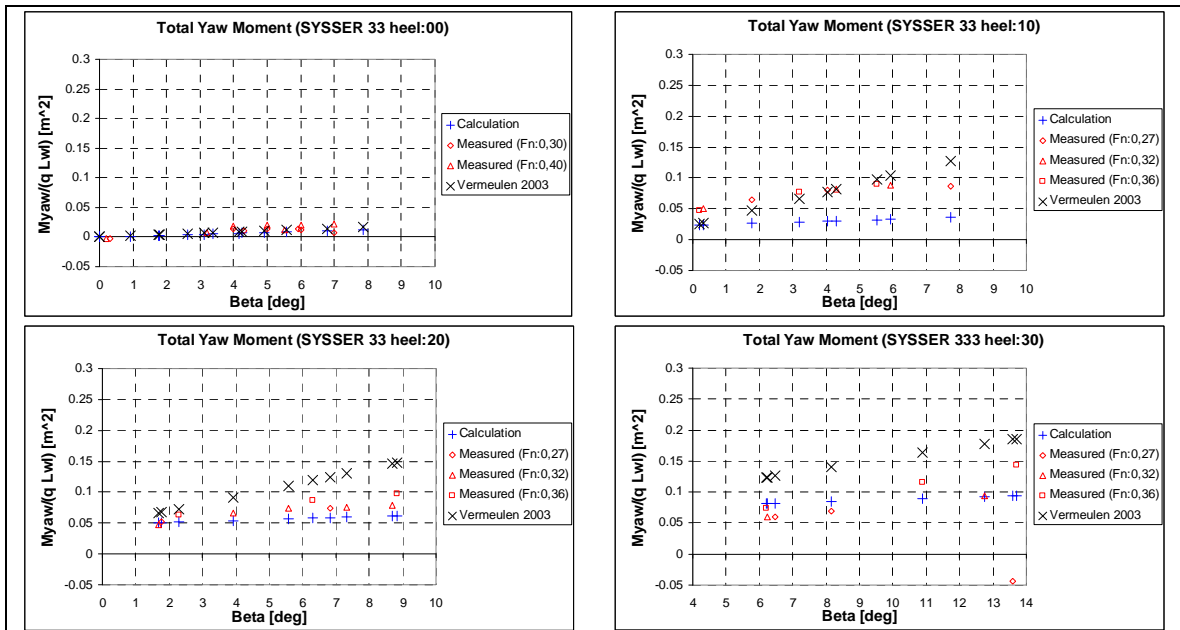


Figure 7: Measured and calculated total hydrodynamic yaw moment vs. leeway for SYSSER 33

3. The Applications

With the dynamic VPP it now becomes possible to investigate the influence of some dynamic phenomena on the performance of sailing boat. These dynamic phenomena may be at present be restricted to fluctuations in true wind strength and true wind direction. The differences between the dynamic solution and the static solution are determined by using the same dynamic VPP but with either a stationary or a fluctuating input. This was done in order to evade possible differences between the customary VPP and the dynamic VPP for the same input. Although by comparison these differences showed to be small some still do exist in particular due to differences in the aerodynamic model. In the following sections all results are presented as differences in distance lost over the distance travelled, presented in percentages, plus meaning distance lost so the boat is slower and minus vice versa.

First it was considered to be of interest to investigate if and how one particular boat is affected by fluctuating true wind strength.

Analyzing some true wind records as obtained from a series of full scale measurements in two different conditions, i.e. close hauled and broad reaching, it appears that a 2 meters per second fluctuation at an average wind speed of around 12-16 knots is not unrealistic. Therefore such an amplitude of the true wind oscillation was selected for this study.

From the same analysis it showed that the “period” of the oscillation depends on the true wind angle: in close hauled condition this period is somewhere around 60 – 70 seconds, in broad reaching condition this is around 200 seconds. This difference between the two conditions can be explained by the fact that broad reaching the gust is followed by the boat so it stays with it for a longer time, while in the upwind condition the opposite holds true. A typical result of such an onboard measurement may be seen in Figure 8 and Figure 9.

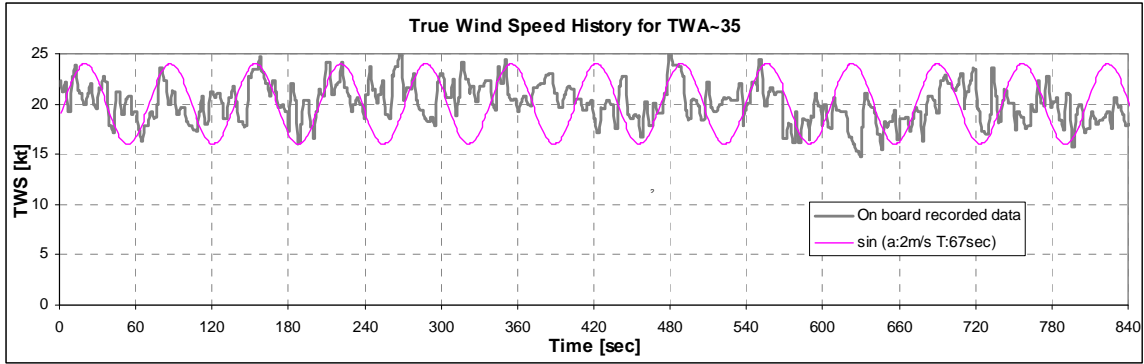


Figure 8: Wind history recorded on board while sailing upwind

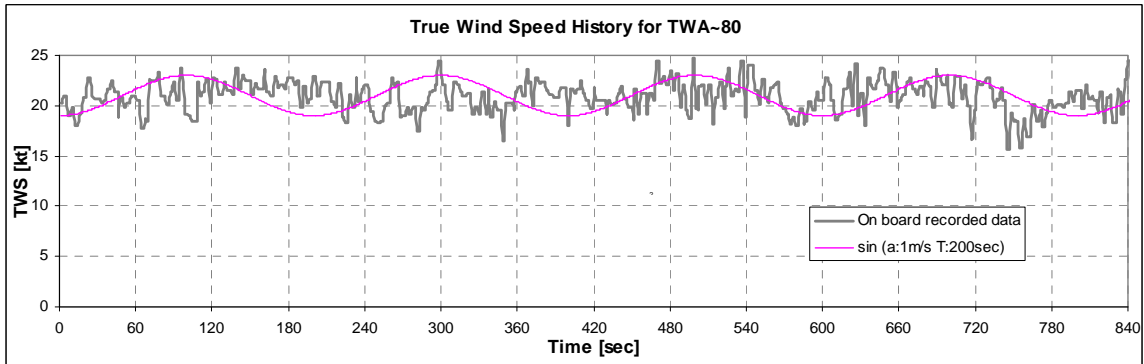


Figure 9: Wind history recorded on board while reaching

What also may be concluded from these records is that there appears a long(er) period fluctuation in the true wind speed, as denoted above, but super imposed on this is a (number of) fluctuations with a significantly shorter period, for these particular records somewhere around 10 seconds and some even shorter. The ultimate approach would be to determine a true wind spectrum, containing all relevant frequencies and amplitudes. In the present study such an attempt has not been made, but instead a simplified approach using a double frequency true wind input signal just to show the effect.

The effort has been made to simulate all these possible scenarios in a more or less systematic way for one particular boat. The main particulars of this boat chosen are presented in Table 1, yacht “b1”. It is supposed to represent a typical contemporary racing boat.

yacht:		b1	b3	b4
		parent	heavy	light
Lwl	[m]	10	10	10
Bwl	[m]	2.5	2.5	2.5
Displ	[m ³]	4.62	10	2.9
Tc	[m]	0.46	0.46	0.46
Sail Area	[m ²]	62.6	62.6	62.6
L/Displ ^{1/3}	[-]	6.00	4.64	7.01
SA/Displ ^{2/3}	[-]	22.57	13.49	30.78

Table 1: Dimensions of the yachts used for the assessment

The different wind scenarios that have been used in the simulations are depicted in Figure 10.

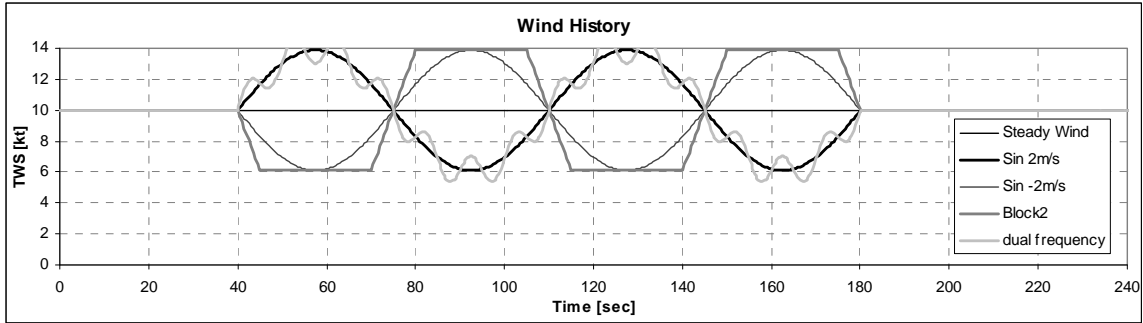


Figure 10: Different true wind scenarios applied

As may be seen here the average wind speed is 10 kts. The amplitude of the fluctuation is 2 m/s. Five different true wind speed scenarios have been used, i.e.:

1. the stationary wind (no change over time)
2. sinusoidal change with amplitude 2 m/s and 70 sec period, starting with an increase
3. sinusoidal change with amplitude 2 m/s and 70 sec period, starting with a decrease
4. a block shaped variation with the same amplitude and period
5. a double frequency harmonic signal with period 1 equal to 70 sec and period 2 equal to 10 sec.

The simulations have been carried out with a true wind angle of 35 and 140 degrees. The autopilot used was the constant true wind angle variant. The respective results of these simulations presented as distance lost using these scenarios are depicted in Figure 11.

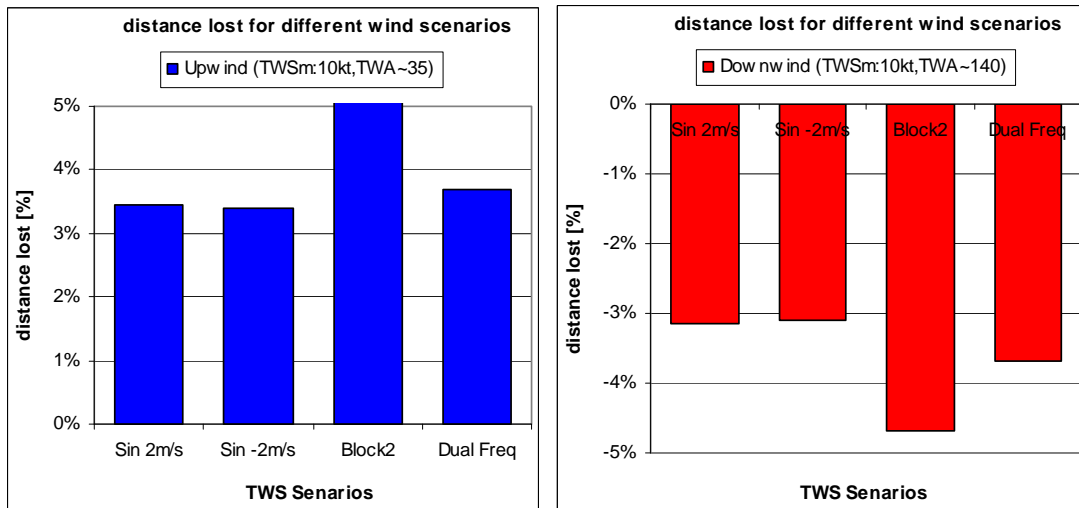


Figure 11: Distance lost in respect to the steady wind scenario for up and downwind course

As may be seen from these results the loss in distance is quite significant, i.e. on average more than 3% of the distance travelled. The biggest loss is with the block shaped gust scenario and amounts some 5%. Apparently the steep flanks of this scenario cause the largest differences. The dual frequency scenario has a larger loss than the pure sinusoidal one, as is to be expected for the same reason. The inclusion of more and / or different periods and amplitudes may lead to further deviations of the purely sinusoidal scenario, but have in the present study not been investigated. Similar results have been found for the condition with 140 degrees true wind angle.

From these results in general it may therefore be concluded that there is a significant difference between the outcome for a steady state true wind and a fluctuating true wind under the given restrictions of autopilot etc. It should be noted however that these differences are of no real interest if all boats are affected in the same way.

This is the reason that the simulations have been extended to three different designs with significantly different weights of displacement. This was considered of interest because a long lasting debate about the difference between heavy and light displacement in this respect has been going on for a long time.

So three different “designs” have been generated and it should be noted that no serious attempt has been made to make it realistic designs. The emphasis was on having boats with very different length displacement ratios. For the sake of simplicity no changes have been made to either sail plan or stability, which makes them from a sailors point of view un realistic designs. The effect of the selected parameters may so be overemphasized. The main particulars of the designs are depicted in Table 1.

To gain more insight in how these different boats are affected by the changing wind speed the following figures have been prepared. In these figures the changing true wind speed, the boat speed, the changing apparent wind angle and the changing driving force for the cyclic wind variation have been plotted for the three different boats.

The first set of graphs (Figure 12) deals with the situation close hauled at 8 knots average true wind speed.

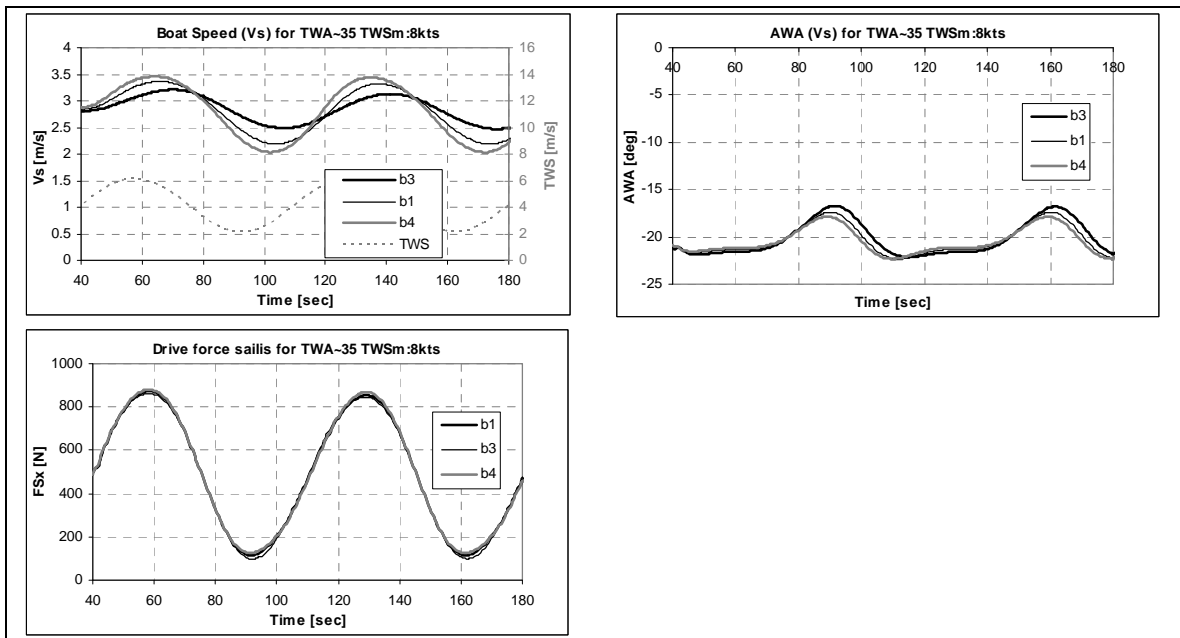


Figure 12: data for close hauled at 8kts average TWS

As may be seen the heavier boat gets a much larger phase shift with respect to the true wind fluctuation than the light boat, meaning she decelerates slower and accelerates slower also, although slightly less. This works out also in the change in apparent wind angle. Due to the large scale the differences between the three designs in the driving force are somewhat masked but the overall change in driving force due to the true wind variations is considerable.

The overall effect of all this is that the lighter boat upwind in light conditions loses more than the heavy boat under the same conditions. The results for downwind in the same wind speed are depicted in Figure 13.

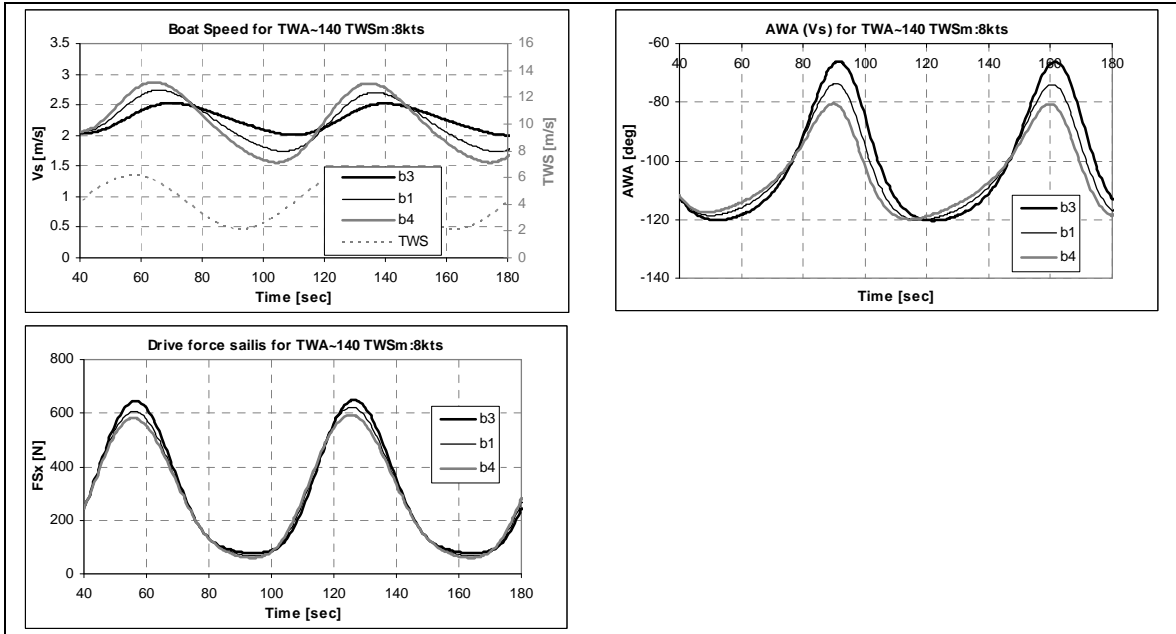


Figure 13: data for downwind at 8kts average TWS

Here the change in apparent wind angle is striking, it amounts almost 60 degrees. Some of the same effects are seen here as mentioned for the upwind case, but in particular the change in the driving force between the designs is significant. Once again the change in apparent wind angle is large in the slow down situation of the boats.

The results for the three different boats in various conditions are shown in the following figures. The first set shows the differences in distance lost for upwind and downwind at relatively low true wind speeds. These results have been reviewed earlier. It shows that the light boat loses more upwind than the heavier boat. In the downwind condition the heavy boat actually gains some distance, while the light boat still loses distance.

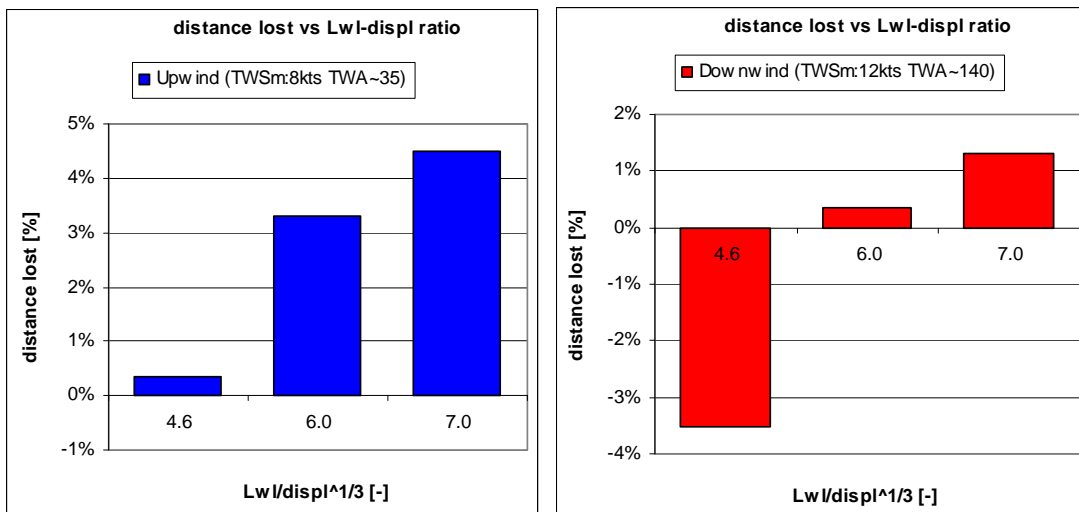


Figure 14: Distance lost for different length-displacement ratios in light winds

In medium range wind conditions (Figure 15) all boats lose: upwind the differences are small, but still the light boat has a disadvantage. Downwind the trend is reversed and shows the light boat a small advantage over the heavier ones.

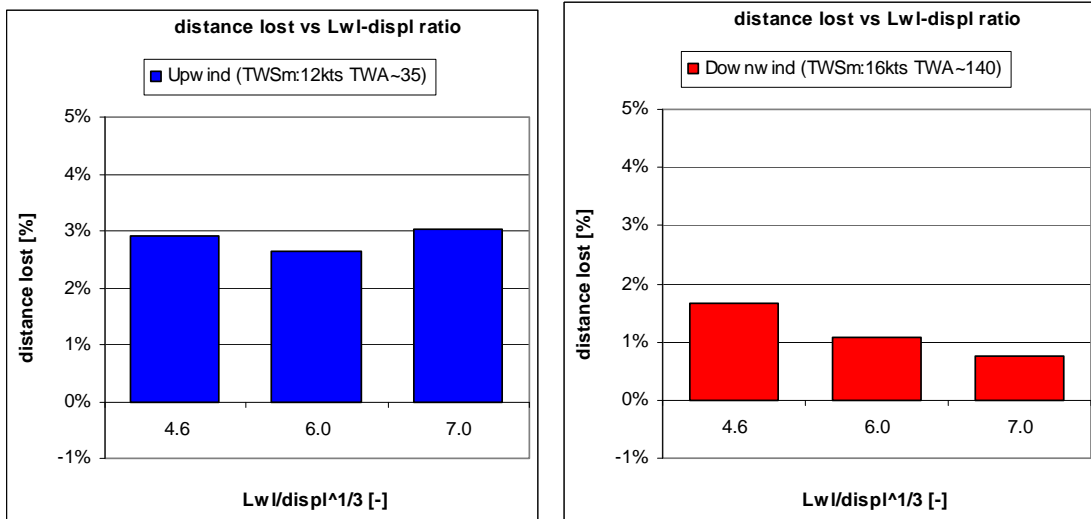


Figure 15: Distance lost for different length-displacement ratios in medium winds

In heavier upwind wind conditions the advantage still is with the heavier boat while downwind the differences are minute, as can be seen in Figure 16.

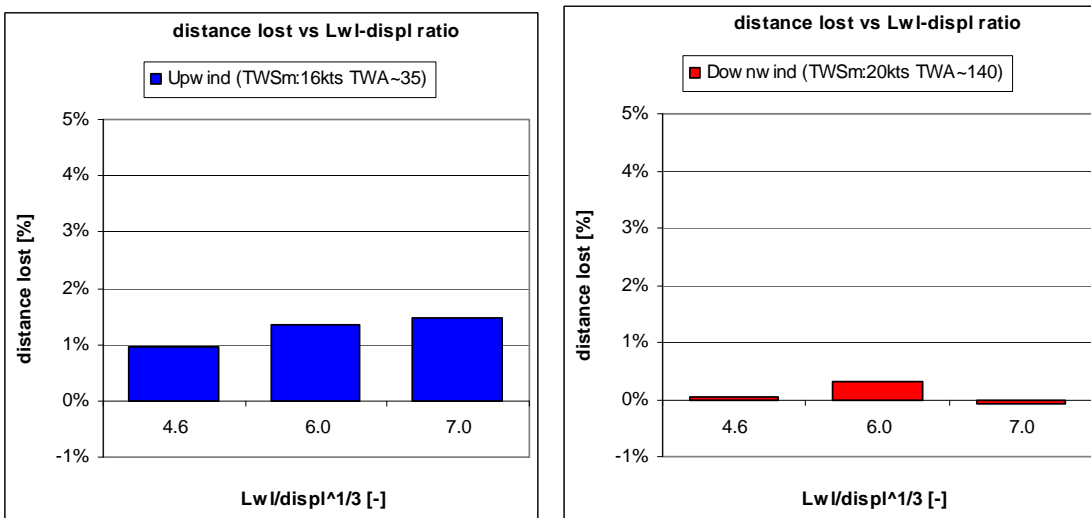


Figure 16: Distance lost for different length-displacement ratios in heavier winds

A few things reviewing these results should be noted here:

First the small difference found in some of the tested conditions may be well within the accuracy band of the calculations and should therefore be considered with some care.

Second in general the effects of waves have not been taken into account. This is one of the foreseen extensions of the dynamic VPP in the future. This holds true for both upwind and downwind conditions. Downwind this implies that no effect of wave surfing has been taken in account. This may lead to much larger differences in downwind conditions in the heavier winds than follows from the present results.

4. Conclusions

The paper shows some results for simulations of sailing yachts under varying conditions. The time domain simulation model that has been derived originally for assessing the maneuvering characteristics of sailing boats offers some attractive alternative applications in this respect.

So it has been used to investigate some of the possible differences between a stationary and a dynamic VPP. Therefore at first approach only a limited number of true wind speed variation scenarios have been used. Although the scope of the present project was restricted and therefore the number of simulations still rather limited some interesting phenomena have been found:

- The actual speed attained under varying more realistic true wind conditions is lower than found in the stationary VPP
- The actual shape of the true wind scenario is of importance
- Different boats are affected differently.
- In general under the conditions tested it was found that heavy boats have the advantage over lighter boats.

In future research further development of the different autopilots is foreseen. Also the adaptation of the aero model in the present model to suite the dynamic behavior more adequately is foreseen. Finally the effect of wind waves should be incorporated, both upwind and downwind.

References

[1]

Keuning, J.A. , Vermeulen, K.J. and de Ridder, E.J.

A generic mathematical model for the manoeuvring and tacking of a sailing yacht.

Chesapeake Sailing Yacht Symposium, 2005

[2]

Keuning, J.A. , Katgert, M. and Mohnhaupt, A.

The use of a maneuvering model for the optimization of the tacking procedure of an IACC sailing yacht.

RINA International conference: The modern Yacht, 2007

[3]

Battistin, D. and Lendri, M.

A tool for time dependent performance prediction and optimisation of sailing yachts.

Chesapeake Sailing Yacht Symposium, 2007

[4]

Gerritsma, J. , Onnink, R. and Versluis, A.

Geometry, resistance and stability of the delft systematic yacht hull series.

HISWA Symposium on Yacht Design and Construction, 1981

[5]

Keuning, J.A. and Vermeulen, K.J.

The yaw balance of sailing yachts upright and heeled.

Chesapeake Sailing yacht Symposium, 2003

[6]

Keuning, J.A. and Sonnenberg, U.B.

Approximation of the Hydrodynamic forces on a sailing yacht based on the Delft Systematic yacht Hull Series.

HISWA Symposium on Yacht Design and Construction, 1998

[7]

Keuning, J.A. , Katgert, M. and Vermeulen, K.J.
Further analysis of the forces on keel and rudder of a sailing yacht.
Chesapeake Sailing Yacht Symposium, 2007

[8]

Whicker, L.F. and Fehlner, L.F.
Free-stream characteristics of a family of low-aspect-ratio, all-movable control surfaces for application to ship design.
Technical report 933, David Taylor Model Basin, 1958

[9]

Keuning, J.A. and Binkhorst, B.J.
Appendage resistance of a sailing yacht hull.
Chesapeake Sailing Yacht Symposium, 1997

[10]

Claughton, A.
Developments in the IMS VPP formulations.
Chesapeake Sailing Yacht Symposium, 1999

[11]

Cambell, I.M.C.
Wind tunnel testing of sailing yacht rigs.
HISWA Symposium on Yacht Design and Construction, 1994

[12]

Ranzenbach, R. and Mairs, C.
Wind Tunnel Testing of Offwind Sails
Chesapeake Sailing Yacht Symposium, 1999

[13]

Fossati, F. , Muggiasca, S. and Viola, I.M.
An investigation of aerodynamic force modeling for IMS rule using wind tunnel techniques.
HISWA Symposium on Yacht Design and Construction, 2006